Nationaal Lucht- en Ruimtevaartlaboratorium
National Aerospace Laboratory NLR

NLR TP 97259

New attempts to solve an old problem: aerodynamic measurements in new vehicle tunnels

A.C. de Bruin, R.A. Maarsingh and L. Swart

DOCUMENT CONTROL SHEET

	ORIGINATOR'S REF.		SECURITY CLASS.
	TP 97259 U		Unclassified

ORIGINATOR
National Aerospace Laboratory NLR, Amsterdam, The Netherlands

TITLE
New attempts to solve an old problem: aerodynamic measurements in new vehicle tunnels

PRESENTED AT
the 9th International Symposium on Aerodynamics and Ventilation of Vehicle Tunnels, Aosta Valley, Italy, 6-8 October 1997

AUTHORS	DATE	pp	ref
A.C. de Bruin, R.A. Maarsingh and L. Swart	970513	26	10

DESCRIPTORS

Anemometers	Transfer tunnels
Flow velocity	Ventilation
Flow measurement	Ventilation fans
Performance tests	Wind effects

ABSTRACT
Prior to the opening of the new Wijkertunnel near Amsterdam on-site aerodynamic measurements were carried out by NLR under contract to the Dutch Ministry of Transport, Public Works and Water Management. Volume flow rates, created at various ventilation conditions, were measured with a SF_6 tracer gas dilution method as well as with conventional anemometer traverses for comparison. For the determination of the resistance of the empty tunnel tube a velocity decay method was adopted. A new power efficiency was defined in order to judge the quality of the longitudinal ventilation system. Rather strong and gusty wind conditions occurred during the two days of the measurements. This required special measures in the analysis of the measurements.

Contents

This page is intentionally left blank.

New attempts to solve an old problem: Aerodynamic measurements in new vehicle tunnels

A.C. de Bruin and R.A. Maarsingh
National Aerospace Laboratory NLR

L. Swart
Ministry of Transport, Public Works and Water Management
The Netherlands

SYNOPSIS

Prior to the opening of the new Wijkertunnel near Amsterdam on-site aerodynamic measurements were carried out by NLR under contract to the Dutch Ministry of Transport, Public Works and Water Management. Volume flow rates, created at various ventilation conditions, were measured with a SF_6 tracer gas dilution method as well as with conventional anemometer traverses for comparison. For the determination of the resistance of the empty tunnel tube a velocity decay method was adopted. A new power efficiency was defined in order to judge the quality of the longitudinal ventilation system. Rather strong and gusty wind conditions occurred during the two days of the measurements. This required special measures in the analysis of the measurements.

List of symbols

p_{bar}	barometric pressure outside the tunnel
p_{in}	static pressure near tunnel entry (Fig. 4)
p_{out}	static pressure near tunnel exit (Fig. 4)
Δp_w	wind induced pressure difference between tunnel portals
u	average air velocity in tuunel
u_a	average velocity at jet fan exit
u_c	average velocity in tunnel, corrected for wind effect (eq. 4.3)
u_d	natural draught velocity due to wind effect
u_k	measured velocity with SF6 tracer gas method
A_a	cross-sectional area of fan exit
A_t	cross-sectional area of the tunnel
D_h	hydraulic diameter of the tunnel

I_a	driving force of jet fans on the tunnel flow
L_p	distance between the tunnel portals
Q_a	volume flow throuhg the jet fan
V_{10}	wind speed at 10 m above the ground
γ_s	wind direction defined in Fig. 5
ζ	total tunnel resistance coefficient
ζ_{in}	entrance loss coefficient defined in Fig. 4
ζ_{out}	exit loss coefficient defined in Fig. 4
λ	tunnel wall friction factor
ρ	air density
η_{tot}	power efficiency defined in eq. 6.4
η_s	power efficiency defined in eq. 6.5
η_{id}	power efficiency defined in eq. 6.8

1. INTRODUCTION

Aerodynamic measurements in newly built road and rail tunnels are needed in order to check both the actual performance and several input parameters used in the design calculation method for the ventilation system (1). Such pressure and velocity measurements involved, make high demands upon measuring methods and techniques, since the measuring conditions are often unfavourable and time is limited. In this paper recent experiences with some unconventional measuring methods are reported, which were applied especially in order to improve the determination of the volume flow rate and the tunnel resistance.

Volume flow rates and mean air velocities were measured with the classical velocity area method (9), using a rotating vane anemometer. In addition a SF_6 tracer gas dilution method (10) was applied. The anemometer and the tracer gas sampling tube were simultaneously traversed across the tunnel section to allow a detailed comparison between the results.

In order to avoid accuracy problems connected with pressure measurements at the low air velocities in a tunnel tube, a velocity decay method was applied to determine the total resistance of the tunnel tube without traffic.

A very important aspect was the presence of a rather strong and variable wind during the two days, June 11 and 12, 1996, allocated for the measurements. As a consequence, quite substantial air velocities (up to 3.3 m/s) occurred in the tunnel in situations without mechanical ventilation. Earlier wind tunnel tests on a model of the Wijkertunnel tunnel portals (3) revealed a rather complex influence of the wind on the portal pressures, similar to the results reported in a previous paper (2). Since the present site measurements require a correction for wind effects some reference will therefore be made to these previous reports.

2. TUNNEL AND VENTILATION CHARACTERISTICS

The Wijkertunnel is a typical Dutch under-water tunnel which consists of two three-lane (13 meters wide and 704 meters long) tubes, each intended for uni-directional traffic. The cross-sectional area of each tunnel tube is 63.9 m^2 and the hydraulic diameter is 7.26 m. Measurements were taken meanly in the east tube.

The longitudinal ventilation system of the east tube consists of six 0.8 m diameter jet fans (outlet velocity ≈ 34 m/s), forming a so-called open injector at the entrance portal. In addition, two groups of four reversible 0.728 m diameter jet fans (outlet velocity ≈ 41 m/s) are suspended in niches from the tunnel ceiling. Figure 1 gives an overall sketch of the tunnel and the location of the ventilators. Details of the open-injector geometry are shown in Figure 2 and the mounting of the other jet fans is presented in Figure 3. As shown in Fig. 2 and 3, deflection vanes were applied at the outlet of the injectors and at the inlet and outlet of the jet fans. Only during part of the tests the jet-fans were operated without deflection vanes.

3. OBJECTIVES AND SCOPE OF THE MEASUREMENTS

The principal objective of the present measurements is the verification of the performance calculation method (see (1), chapter 12), under various ventilation conditions. This requires the determination of: inflow and outflow loss coefficients, wall friction factor, volume flow-rate and power efficiencies.
Additional aims were:

- the determination of the effects of the jet fan deflection vanes on the capacity of the ventilation system
- a comparison of velocity and volume flow results of vane anemometer and SF_6 tracer gas dilution method.
- a comparison of the present test results with wind tunnel measurements on a scale model of the portals of the Wijkertunnel (3).

4. PROBLEMS DUE TO WIND

During the two days of the measurements rather strong winds occurred. At a nearby weather station (Schiphol Airport) the mean (10-minutes averaged) wind speed V_{10} (at 10 m height) was between 4 and 7 m/s, with occassional peak values up to 12 m/s. As a consequence, quite substantial draught velocities (up to 3.3 m/s) occurred in the tunnel and, with ventilation velocities between 4 and 9 m/s, the wind effects cannot be ignored.

Before considering the wind effects in detail we consider the condition without wind. Figure 4 gives a schematic presentation of the total and static pressure distribution along the tunnel axis. It has to be remarked that Fig. 4 shows a condition with boosters at mid-tunnel position, but the concept also applies to any other longitudinal ventilation arrangement. The friction, inflow and outflow losses are introduced step by step in Fig. 4a to 4c. As shown in Fig. 4d, the far ends of the tunnel are considered separately from the central part of the tunnel. In the central part with length L_p the flow velocity distribution across the tunnel section becomes reasonably well developed. Also the pressure become reasonably uniform across the tunnel cross-section and the streamwise pressure gradient is entirely due to friction losses. Experience shows that (depending on entrance and exit shaping) a distance from the tunnel ends of about 10 hydraulic diameters is needed, so $L_p \approx L-20D_h$.

With ventilation system switched on, and in the presence of wind, the force balance equation for the steady flow in an empty tunnel tube can then be written as:

$$\left|\Sigma I_a + \Delta p_w A_t\right| = (\zeta_{in} + \zeta_{out} + \lambda L_p/D_h)(\rho u^2/2) A_t,$$
$$\zeta_{in} = \frac{(p_{bar} - p_{in})}{\frac{1}{2}\rho u^2} - 1, \quad \zeta_{out} = \frac{(p_{out} - p_{bar})}{\frac{1}{2}\rho u^2} + 1 \qquad (4.1)$$

where p_{in} and p_{out} should be (understood to be) determined without wind, Δp_w is the wind-induced pressure difference between the portals, ΣI_a is the actual or apparent total driving force of the fans in operation, $\zeta_{in} + \zeta_{out}$ is the sum of inflow and outflow loss coefficients and includes the friction losses over the outer parts of the tunnel (see Fig. 4d), λ is the wall friction coefficient, u the *average* velocity and A_t is the cross-sectional area, L_p the length between the locations where p_{in} and p_{out} are measured and D_h the hydraulic diameter of the tunnel tube. Δp_w and ΣI_a are considered to be positive when acting in normal ventilation direction (from South to North). It has to be noted that wind effects are entirely represented by Δp_w and do not influence ζ_{in} and ζ_{out} *which are to be determined under no-wind conditions*.

In a steady condition without mechanical ventilation, $\Sigma I_a=0$ and $u=u_d$ (natural draught velocity), the force balance becomes:

$$\left|\Delta p_w\right| A_t = (\zeta_{in} + \zeta_{out} + \lambda L_p/D_h)(\rho u_d^2/2) A_t \qquad (4.2)$$

Conventionally, it is assumed that $\Delta p_w = C_2^* . \rho V_{10}^2/2$ and thus independent of ventilation velocity u, so that equation 4.2 can be substituted into 4.1, and the result can be considered to express a situation corrected for wind:

$$\left|\Sigma I_a\right| = (\zeta_{in} + \zeta_{out} + \lambda L_p/D_h) * (\rho u_c^2/2) * A_t, \quad \text{where } u_c = \sqrt{u^2 \pm u_d^2} \qquad (4.3)$$

Here u_c is the mean velocity corrected for wind effect (the + and - signs correspond with a natural draught in the opposite and in the same direction as the velocity u, respectively).

In a previous paper (2) it was pointed out already, that the assumption of a constant Δp_w (invariant with mean velocity u) is fundamentally incorrect and the wind correction derived above is questionable. Unfortunately, in the present site measurements only static pressures at the inflow side of the east tube were measured and Δp_w could not be evaluated therefrom. Tests on a 1:200 scale model of the (northern) portal of the Wijkertunnel in the NLR low-speed wind tunnel (3), allowed an independent variation of tunnel velocity, wind speed and wind direction. It was found that for a condition without wind $\zeta_{in}+\zeta_{out} \approx 1.5$ and that for normal ventilation direction ($u>0$) the wind induced pressure difference between the tunnel portals can be approximated as:

$$\Delta p_w \approx \left[(C_1(u/V_{10}) + C_2)(V_{10}/u)^2\right]\rho/2\,u^2,$$
$$\text{with:} \quad C_1 = 0.16\cos^2\gamma_s - 0.12\cos\gamma_s - 0.345, \tag{4.4}$$
$$C_2 = -0.02\cos^2\gamma_s + 0.73\cos\gamma_s - 0.02,$$

where γ_s is the wind direction with respect to the southern portal axis (Fig. 5). The formula has been written with the $(V_{10}/u)^2$-term between brackets to express the relative importance of the Δp_w term in equation 4.1.

The first term on the right hand side is due to an *interaction between the internal flow and the external wind*, its contribution depends primarily on u/V_{10} and only weakly on wind direction (see Fig. 6). The second term is due to the direct action of the wind and depends of coarse on the wind direction γ_s (see Fig. 6). The traditional wind correction, equation 4.3, does not account for the interaction term.

For low u/V_{10} values the second term will dominate, but for u/V_{10} values near unity (as occurred in the present site experiments with mechanical ventilation switched on or shortly after shut down) the first term may partly balance the contribution of the second term, depending on flow direction γ_s. Application of equation 4.4 to the volume flow rate measurements with forced ventilation (taking average wind conditions from nearby Schiphol weather station), indicates that only small velocity corrections are required (smaller or at most equal to the simple correction procedure of equation 4.3). Unfortunately, in the absence of precise local wind data, a reliable exploitation of the wind tunnel test results for the data reduction of the present site measurements is not possible and it must be accepted that the data can not be fully corrected for wind effects. Also, with all measurements taken during strong wind conditions, the sum of the inflow and outflow losses could not be determined. According to Fig. 4 it must be larger than unity. The wind tunnel measurements indicate a value near 1.5, but since the actual tunnel entrance geometry is somewhat different from the wind tunnel entrance geometry (in order to accomodate the injectors, see Fig. 2), the actual inflow loss coefficient might be smaller than in the windtunnel experiment, say $1.0<\zeta_{in}+\zeta_{out}<1.5$.

Finally, it should be remarked that site measurements in strong (steady) wind conditions can also have an advantage, as can be seen after rewriting equations 4.1 and 4.2 in the following forms:

$$\left|\Sigma I_a/A_t + \Delta p\right| = (\lambda L/D_h)(\rho u^2/2), \tag{4.5}$$

$$\left|\Delta p_d\right| = (\lambda L/D_h)(\rho u_d^2/2), \tag{4.6}$$

where Δp and Δp_d are the resultant pressure differences between the portals p_{in}-p_{out} (including inflow and outflow losses) with ventilation on and with ventilation off, respectively. The friction loss coefficient λ can be determined directly from equation 4.6, provided that Δp_d and u_d are measured. By substituting that value of λ in equation 4.5 and measuring u and Δp again, the actual thrust of the fans ΣI_a is obtained. Unfortunately, the above method could not be used here since only the pressure at the inflow side of the tunnel was measured.

5. MEASUREMENTS

The locations where the measurements were taken are shown in Fig. 1. Measurements were made mainly in the east tube of the tunnel. The table on the next page gives a survey of the measured and derived quantities.

The barometric pressure outside the tunnel served as a reference pressure for the static pressures measured at the tunnel side walls at 75 m from the tunnel entrance. A special test setup (see (4) for the details) and the usage of a 10 litre isolated pressure vessel, prevented fluctuations of reference pressure due to (unsteady) wind effects.

A velocity decay method was adopted for the determination of the total flow resistance of the empty tunnel tube, i.e. the sum of the wall friction and inflow and outflow losses. The velocity decay method has been proposed several times by other investigators (5-8), but as far as we know, has never been applied as an operational technique. The method requires the measurement of the mean air velocity in the tunnel tube as a function of time after shut-down of the mechanical ventilation. Mainly for that purpose, but also in an attempt at simplifying the volume flow-rate measurements, a so-called reference velocity was measured continuously during all measuring conditions. The reference velocity u_{ref} has been defined as the mean value calculated from the air velocities measured with three vane anemometers in a cross section 10 meters upstream of the tunnel cross-section where the full velocity traverse was made (see Figs. 1 and 7). These vane anemometers were in fact combined velocity/temperature probes.

denomination of quantities	measured	derived	
static pressures (at tunnel entrance)	p_3, p_4	$p_{in}=(p_3+p_4)/2$	[N/m^2]
barometric pressure (outside of tunnel)	p_{bar}	p_{bar}	[N/m^2]
reference velocities	u_1,u_2,u_3	$u_{ref}=(u_1+u_2+u_3)/3$	[m/s]
temperature (mass density of air)	t_1,t_2,t_3	$t=(t_1+t_2+t_3)/3$ $\rho=3.468 \times p_{bar}/(273+t)$	[° C]
velocity in 30 grid points (traverse section)	u_i	$u=\sum_{i=1}^{30} u_i/30$	[m/s]
SF_6-samples in 30 grid points (volume flow rate)	C_{SF6} [ppb] q_{SF6} [m^3/s]	$Q=q_{SF6}/C_{SF6}$ $u=Q/A_t$	[m^3/s] [m/s]
natural draught in west tube (corrected mean velocity)	u_w (west) (sign + or -)	u_e (east) $u_c=\sqrt{(u^2 \pm u_e^2)}$	[m/s]
electrical power consumption (taken from mains)	P	ΣP (for power efficiency)	[kW]

The average velocity was determined by traversing a rotating-vane anemometer over a tunnel cross-section at 60 m from the tunnel exit. The 30 measuring locations were distributed

such as to follow closely a log-Tchebycheff (9) distribution of gridpoints (see Fig. 7b). Therefore the average velocity is equal to the arithmetic mean of the thirty measurements, with good approximation. The unsteady character of the flow required averaging of the signals during at least half a minute per measuring point. A full velocity traverse requires about 40 minutes. During that period the local wind conditions may change considerably and it becomes necessary to apply a time-dependent correction for the wind effects.

As an alternative for the elaborate vane-anemometer measurements use of a SF_6 tracer gas dilution method (10) has been attempted. The SF_6 tracer gas was injected (with a known flow-rate q_{SF6}) at four points at 75 m from the tunnel entrance (see Fig. 1). The SF_6-concentration samples (C_{SF6}) were taken simultaneously (and at the same locations) with the vane-anemometer traverse. In case of fully homogeneous mixing of the tracer gas over the tunnel cross-section the air volume flow rate Q can directly be computed as $Q=q_{SF6}/C_{SF6}$ and the velocity is obtained from $u_k=Q/A_t$ (the subscript k is added to distinguish the velocity from that obtained from the vane anemometer). In practice the mean flow velocity was obtained by averaging over the 30 measuring points. Also some velocity decay measurements were made, with the sampling tube placed at a fixed position in the middle of the tunnel cross-section.

The variable external wind conditions were a point of concern. With the present measurements taken in the east tube, it was decided to monitor continuously the natural draught velocity u_w with a vane anemometer placed in a mid-tunnel position in the adjacent west tube. The flow direction was recorded with a wind vane. These data were used in a simplified correction procedure for wind effects.

Finally, in order to evaluate the efficiency of the ventilation system, the electric power consumption of three jet fans (one out of each of the three groups of jet fans) was measured.

6. RESULTS

6.1 Natural draught velocities in both tunnel tubes

Local wind conditions were not measured but external wind data could be made available from a weather station at Schiphol Airport (about 18 km from the Wijkertunnel). It seems interesting to make a comparison between these 10-min. mean values of the external wind and the measured draught velocities in both tunnel tubes. The results are summarized in Fig. 8 for the two measuring days separately.

On the first day (Fig. 8a) the wind blew obliquely into the southern portals (SW to W, see Fig. 5), creating a natural draught from South to North, whereas on the second day (Fig. 8b) the wind blew rather into the northern portals (W to NNW, see Fig. 5), resulting in a natural draught from North to South, in the east as well as in the west tube.

It can be observed that:

- On June 11 all the velocities, i.e. u and u_{ref} in the east tube and also u_w in the west tube, have almost the same values, whereas on June 12 u_w sometimes differs significantly from u and u_{ref} in the east tube.
- On June 11 all velocities in the tunnel seem to correlate with the 10-minutes mean external wind velocity V_{10} to such an extent, that u_w, u and u_{ref} are mostly equal to about $V_{10}/3$.
- On June 12 the natural draught velocities are much more variable (between 0.4 and 3.3 m/s) and correlation with V_{10} seems to be poor, presumably because the wind direction is sometimes perpendicular to the portal axes.

As could be expected, the reference velocity u_{ref} is not exactly equal to the mean velocity u.

A mean value of the ratio $u/u_{ref} \approx 0.92$ was found. In spite of the objections, made in section 4, to the conventional wind correction, this correction has been applied for the time being, taking $u_d \approx u_w$ on June 11 and $u_d \approx 1.3$ to $1.5u_w$ on June 12.

6.2 Mean velocities and flow rates in various ventilation conditions

From the vane anemometer traverses the following results, corrected for wind effect, have been obtained:

run	ventilation		mean velocity u_c [m/s]	flow rate Q [m^3/s]
	direction	condition		
2	normal	open injector (6J)	5.9	376.9
4	normal	two groups of jet fans (4Z+4N)	6.2	396.1
7	normal	injector + jet fans (6J+4Z+4N)	8.4	536.6
12	normal	one group of jet fans (4Z)	4.4	281.1
17	normal	one group of jet fans (4N)	4.5	287.5
26	normal	ditto, deflection vanes off	3.7	236.4
33	reversed	two groups of jet fans (4Z+4N)	6.4	408.8

From this it is concluded that:
- The ventilation performances of the southern (4Z, run 12) and the northern group (4N, run 17) of jet fans are similar.
- When both the southern and the northern group of jet fans are in operation (runs 4 and 33), i.e. when the ventilation capacity is doubled, the mean velocity u_c approximately increases by a factor $\sqrt{2}$, in agreement with theory ($u_c \div \sqrt{(\Sigma I_a)}$, see equation 4.3).
- The ventilation capacity of the open injector (run 2) is close to that of both groups of jet fans in operation (run 4 or 33). Therefore, with the complete system switched on (run 7), the mean velocity is almost $\sqrt{2}$ times the value obtained with both the southern and northern group of jet fans in operation.
- Due to the application of deflection vanes on the jet fans the ventilation capacity increases by about 20 % (compare run 17 and 26).
- Reversal of ventilation direction does not seem to affect the ventilation capacity of the jet fans significantly.

More details about the ventilation performances will be given in section 6.5.

6.3 Comparison of tracer gas and anemometer traversing method

Since both kind of measurements have been made simultaneously, no wind correction is needed to compare the results.

run	ventilation condition	measured mean velocity	
		anemometer u [m/s]	SF_6-tracer u_k [m/s]
7	injector plus jet fans (6J+4Z+4N)	8.6	8.18±0.22
12	southern group of jet fans (4Z)	5.0	5.67±0.18
17	northern group of jet fans (4N)	4.8	5.36±0.10

Apparently in runs 12 and 17 the tracer gas results are 12 to 13 % higher than those of the conventional method, whereas in run 7, with all fans in operation, they are 5% lower. For the SF_6-results uncertainty margins have been indicated. It is known that unsteady flow effects may lead to an over-prediction of anemometer velocities, but this can not explain the observed differences for run 12 and 17. The smaller disagreement for run 7 could be explained perhaps by a better mixing due to the highly turbulent jets from the injectors just upstream of the location where the tracer gas was injected (see Fig. 1).

Figure 9 shows a typical example of the measured velocities during a traverse run. By reference to Fig. 7 the anemometer results indicate low velocities in the corners and close to the tunnel walls. The results derived from the local SF_6 tracer gas concentrations show a similar, though weaker, regular pattern as the anemometer results. Therefore the tracer gas is apparantly not yet fully mixed. Yet, averaging the 30 samples (as was done here), one would expect to obtain a reliable value for the mean velocity. For the time being the differences between the mean anemometer and tracer gas velocities are not explained.

6.4 Velocity decay measurements

The velocity decay, that occurs after the mechanical ventilation has been switched off, depends on the total resistance of the tunnel. The unsteady motion of the tunnel flow is given by the following equation:

$$\pm\Delta p_w - \zeta\frac{1}{2}\rho u^2 = \Delta p - \lambda L_p/D_h\,\frac{1}{2}\rho u^2 = \rho L\frac{du}{dt}, \qquad (6.1)$$

where Δp_w is the pressure difference between the "tunnel portals" (see Fig. 4) due to wind only, Δp is the total (resultant) pressure difference between the "tunnel portals" (see Fig. 4), $\zeta=\zeta_{in}+\zeta_{out}+\lambda L_p/D_h$ is the sum of all (inflow, outflow and wall friction) resistance coefficients, L is the total length of the tunnel tube, L_p the distance between the "tunnel portals" and u is the instantaneous mean air velocity in the tunnel tube. It should be noted that the "total resistance" coefficient ζ can be obtained provided that Δp_w is known. On the other hand the friction coefficient λ can be obtained provided that Δp is measured as function of time. Unfortunately Δp was not measured during the present experiments.

Substitution of the Δp_w models that were introduced in section 4, yields:

$$\begin{aligned}\left[C_1(V_{10}/u) + C_2(V_{10}/u)^2 - \zeta\right]\rho u^2/2 &= \rho L du/dt\\ \left[C_2^*(V_{10}/u)^2 - \zeta\right]\rho u^2/2 &= \rho L du/dt\end{aligned} \qquad (6.2)$$

At the end of the decay the left hand side terms between brackets must become zero. This can only be satisfied for a certain value of V_{10}/u. The final draught velocity will thus be

proportional to the wind speed V_{10}, the constant of proportionality depends on ζ and wind direction γ_s. The simplified model for Δp_w predicts a relatively low influence of wind on du/dt for high u, but this is not necessarily the case with the extended Δp_w model.

With the simplified model for Δp_w, and assuming that wind speed and direction remain constant during the decay, Δp_w = constant and equal to its end value $\Delta p_w = \zeta \rho u_e^2/2$. Integration of equation (6.1) then yields:

$$u(t) = u_e \frac{e^{a+bt}+1}{e^{a+bt}-1} \quad \text{or :} \quad \ln\frac{u(t)+u_e}{u(t)-u_e} = a+bt, \qquad \text{where:} \quad a = \ln\frac{u_0+u_e}{u_0-u_e}, \quad b = \zeta u_e/L \tag{6.3}$$

In this equation u_0 is the value of u at t=0 (where u starts to decrease after shut down of the mechanical ventilation) and u_e is the final natural draught velocity. The constant "a" follows directly from u_0 and u_e. The constant "b", and so ζ, was determined from a linear regression with "zero y-intercept". The time interval was limited to the first 60 sec of decay. Alternatively ζ was also obtained from equation 6.1, by fitting u=u(t) and estimating du/dt_0 at the beginning of the decay. The results are given in the following table.

run	u_0 [m/s]	u_e [m/s]	ζ eq. 6.1 du/dt_0	ζ eq. 6.3 lin. regr.
5	7.1	1.8	2.0	2.0
8	9.2	3.3	1.6	2.5
13	5.8	2.0	2.3	2.7
34	7.0	3.3	1.6	2.5

Due to the variations in u(t) caused by the wind and possibly also because u_{ref} instead of the true average velocity u was used, a substantial variation in ζ values is observed. The results obtained from linear regression are probably more consistent than those based on du/dt_0. For Reynolds numbers between 1 and $5x10^6$ ($2 < u < 10$ m/s) for smooth pipe flows: $.0090 < \lambda < .0116$ and $.78 < \lambda L_{out}/D_h < 1.0$ ($L_{out} = L - L_{in}$, L_{in}=75 m). With $\zeta_{in}+\zeta_{out}$ between 1 and 1.5 one should therefore expect a lower limit value for ζ between 1.8 and 2.5, which is close to the present values and suggests that the tunnel walls of the Wijkertunnel are quite smooth. It is also clear that, for a relatively short tunnel like the Wijkertunnel, the friction term constitutes only a small part of the total tunnel resistance. In the following ζ=2.5 is assumed but it must be noted that this is only a general assessment.

6.5 Ventilation efficiencies

The flow through the tunnel is accompanied by several energy losses. Some of the losses are inherent to the flow through an open ended conduit and other losses are due to an inefficient energy transfer from the jet fans to the tunnel air. Assuming for the time being that the jet fans transfer their energy to axial kinetic energy of the tunnel flow *without any additional*

losses at the jet fans and recall the force balance introduced in section 4 and explained in Fig. 4. It is clear that the ventilation system must deliver $\Sigma I_a.u_c$. With ΣI_a defined by equation 4.3 the required power is due to three terms:

- The energy required for the acceleration of the air: $A_t u_c.\rho u_c^2/2$.
  This term can be associated with the exit loss coefficient $\zeta_{out}=1$ and it is unavoidable for a flow through an open channel where the axial kinetic energy is entirely lost at the exit.
- The energy required for the inflow losses at the tunnel entrance: $A_t u_c \zeta_{in}.\rho u_c^2/2$.
  This term can be minimized by optimal shaping of the tunnel entrance ($\zeta_{in}\downarrow 0$).
- The energy required to overcome the friction losses: $A_t u_c.\lambda L/D_h.\rho u_c^2/2$ where λ depends on Reynolds number Re_{Dh} and on the roughness of the tunnel walls, it can be minimized by applying smooth tunnel walls.

The sum of these three terms $\Sigma I_a.u_c$ can be considered as the minimum required power of the ventilation system for a given tunnel geometry.

The following definition of the power efficiency is often (see (1) and (4)) used for longitudinal ventilation systems:

$$\eta_{tot} = \frac{A_t u_c(\rho u_c^2/2)}{\Sigma P \times 1000} \tag{6.4}$$

This definition is thus based on the kinetic energy loss of the flow leaving the tunnel exit, divided by the electrical power ΣP (kW) taken from the mains. A power efficiency that takes into account also the tunnel entry and friction losses is:

$$\eta_s = \frac{\Sigma I_a u_c}{\Sigma P \times 1000} = \eta_{tot}(\zeta_{in}+\zeta_{out}+\lambda L/D_h) = \eta_{tot}\zeta, \tag{6.5}$$

It differs from the ventilation efficiency η_{tot} only by the factor ζ which explains why the simple formula for η_{tot} can still be useful to compare tunnels of about similar shape and length. It must however be noted that for the present Wijkertunnel ζ is about 2.5, but that this factor may be much larger for long rough-walled tunnels and for such tunnels the usage of equation 6.4 will lead to very low η_{tot} values. Assuming ζ=2.5 for the moment very low values for the tunnel efficiencies η_{tot} and η_s are obtained (see table below). The efficiencies η_{id} and η_p will be defined later on.

run	ventilation condition	u_c/u_a	η_{tot} (%)	η_s (%)	η_{id} (%)	η_p (%)
2	open injector (6J)	0.17	7.0	17.5	29(34)	60(51)
12,17,24	4 jet fans in operation	0.11	4.0	10.0	20	50
26	ditto, deflection vanes off	0.09	2.3	5.8	16	36
4,23	8 jet fans in operation	0.15	5.3	13.3	26	51
30	ditto, deflection vanes off	0.13	4.0	10.0	23	43

Apparently, the transfer of energy from the jet fans to the tunnel flow involves very large additional losses. To explain this, the energy transfer of the jet fans to the tunnel flow is

considered in more detail. Suppose that u_a is the average velocity in the outlet of the jet fan and the volume flow through the outlet is $Q_a=u_aA_a$. With the fan placed in air with velocity u ($u \ll u_a$), the theoretical transfer of energy to the tunnel air (4) is equal to:

$$I_{theor}u = \rho u_a Q_a(1-u/u_a)u, \tag{6.6}$$

whereas the power output of the jet fan is:

$$\rho Q_a(u_a^2-u^2)/2 \tag{6.7}$$

Therefore the ideal power efficiency of a jet fan becomes:

$$\eta_{id} = \frac{\rho u_a Q_a(1-u/u_a)u}{\rho u_a^2 Q_a(1-u^2/u_a^2)/2} = \frac{2u/u_a}{1+u/u_a}, \tag{6.8}$$

For the present jet fans $u_a \approx 41$ m/s (for the injectors $u_a \approx 34$ m/s) and with tunnel velocities as low as 4 to 8 m/s, u/u_a is only 0.1 to 0.2 and fan power efficiencies of only 18 to 33% should be expected, even under "ideal" conditions. For given ventilation speed u the power efficiency of the fans can only be improved by reducing u_a. However, in order to maintain the same thrust, the fan diameter must be increased approximately in proportion with $1/u_a$, which in view of the limited space available is not possible in most longitudinal ventilated tunnels. If one accepts this constraint and the poor energy transfer of the ventilator (even under "ideal" circumstances), it seems improper to use ΣP in the denominator of η_{tot} and η_s. Instead, it would be much more appropriate to use the product $\Sigma P\eta_{id}$ (the propulsive power that can be transfered to the tunnel flow under ideal circumstances). Therefore, a *new power efficiency* $\eta_p = \eta_s/\eta_{id}$ is proposed.

The potential advantage of the new definition is easily shown. Suppose that a longitudinal ventilation system consists of identical jet fans, that can be switched on individually. Then, when n is the number of jet-fans in operation, it follows from equation 4.3 that to a good approximation $u_c \propto \sqrt{n}$ and $\Sigma P \propto n$. Therefore the following relationships approximately apply: η_{tot} and $\eta_s \propto n.\sqrt{n}/n = \sqrt{n}$ and $\eta_{id} \propto u/u_a \propto \sqrt{n}$. On the other hand η_p remains independent of n and can be used as a criterion for the quality of the longitudinal ventilation system. According to the values shown in the table above the ventilation efficiency η_p is about 51 % (with estimated value $\zeta \approx 2.5$), but becomes much less for cases without deflection vanes.

The results for run 2, where the injector fans were in operation, deserve some discussion. Since the injector fans protrude from the tunnel mouth, where $u \approx 0$ (Fig. 2), it seems appropriate to replace formula 6.8 by:

$$\eta_{id} = \frac{\rho u_a Q_a}{\rho u_a^2 Q_a/2}u = 2\ u/u_a.$$

With this modification the values between parentheses are obtained, which seem to be more plausible than the other values obtained when formula 6.8 is applied.

Selection of a proper local effective velocity u at the fan, to be used in equation 6.8, might be a problem (especially for highly asymmetrically placed jet fans). This might limit the applicability of the new power efficiency η_p in practice. Nevertheless, the above analysis might be seen as a warning against comparing power efficiencies for tunnels with different length and/or ventilation velocities.

It should be noted that the overall ventilation efficiency $\eta_p \approx 50$ % is still rather low. The following (possible) causes can be mentioned:

- The energy transfer of the jet fans to the tunnel flow is not ideal, there are additional losses at the fan entrance, at the fan itself and inside the fan housing. There may be also a residual swirl of the flow at the fan exit and there are heat losses in the electro motor that drives the fan.
- The flow in the tunnel is considerably disturbed in the near region of the fan by the contracting streamtube that enters the fan. This not only disturbes the flow that by-passes the fan but may also lead to high wall friction in a region just upstream of the fan.
- The high velocity jet may scrape over the tunnel walls and induce high wall friction losses locally. This will certainly have an important effect when there are no deflection vanes.

7. CONCLUSIONS

Provided that appropriate precautions are taken, (steady) windy conditions need not necessarily prevent site measurements of the type considered in this paper. A prerequisite for a correct interpretation of the results obtained in such conditions is that static pressures are measured at both far ends of the tunnel tube in question. In case of two separate adjacent tunnel tubes the natural draught (as well as static pressures) should be measured in the adjacent tube to allow a correction for wind effects. Especially when the results are compared with data from model experiments, the local external wind conditions should be known properly. Wind data recorded at a nearby weather station may be useful but will induce some uncertainty. If the wind is strong and unsteady, with large variations in windspeed and direction, this may prevent a consistent set of data from being obtained.

The differences found between the results of the anemometer and the tracer gas measurements could not yet be explained conclusively. The method of sampling as applied in this investigation, where 30 grid points were passed along in succession, may not be optimal. Because of the potential advantages of the tracer gas technique, it will be applied (with some adaptations in the test setup) again in future measurements. On the other hand, the mean velocities measured by means of the conventional anemometer traverse method, corrected for wind effect, seem to represent a consistent set of data, although inaccuracies of unknown magnitude may be present due to flow unsteadiness.

The velocity decay method yielded valuable information, but due to the variable and strong wind the experimental scatter was large. It will be explored further in future measurements, if possible also in low wind conditions and in combination with the tracer gas dilution method.

The total resistance of the Wijkertunnel seems to be rather low (close to what must be expected for a smooth-walled pipe flow). It was noted however that the power consumption of the jet fans was between 6 and 10 times the energy that would be required to balance the resistance of the tunnel flow. It was observed that the power efficiency improved as the tunnel velocity increased. A close inspection of the ideal energy transfer of the jet fan to the tunnel flow reveals a poor fan performance due to the fact that the outflow velocity of the fans is much higher than that of the ambient tunnel air. A new power efficiency was defined that takes into account these losses. Even so, the power efficiency of the ventilation system remains rather poor (around 50 %), indicating that there are substantial additional losses. In a new research project it will be attempted to improve the energy transfer of the jet fans to the tunnel flow.

8. REFERENCES

1. Swart, L. et al., Ventilation of road tunnels. Recommendations 1991. Royal Institute of Engineers (KIVI), Working Party Ventilation of Road Tunnels, Ministry of Transport, Public Works and Water Management, Civil Engineering Division, Feb. 1994.
2. Maarsingh, R.A., and Swart, L., Wind-tunnel experiments on wind effects at tunnel portals. Paper presented at the 7th International Symposium on Aerodynamics and Ventilation of Vehicle Tunnels, Brighton, UK, Nov. 1991.
3. Maarsingh, R.A. and Bakker, L.G., Wind-tunnel experiments to determine wind-induced pressures at tunnel portals on the basis of a scale model of the Wijkertunnel (In Dutch). NLR Report CR 92037 L, Feb. 1992.
4. Maarsingh, R.A. and Kamp, A., van der, Aerodynamic measurements in the Wijkertunnel. NLR report CR 96664 L, Oct. 1996.
5. Baba, T. et al., Characteristics of longitudinal ventilation system using normal size jet fans. Paper presented at 3rd Int. Symp. on Aerod. and Vent. of Veh. Tunnels, Sheffield, England, March 1979.
6. Baba, T. et al., Aerodynamic specialities in connection with the Tsuruga tunnel. Paper presented at 4th Int. Symp. on Aerod. and Vent. of Veh. Tunnels, York, U.K., March 1982.
7. West, A. and Pope, C., Wind induced flow and resistance measurements in a rock hewn tunnel. Paper presented at 5th Int. Symp. on Aerod. and Vent. of Veh. Tunnels, Lille, France, May 1985.
8. Landolfa, A. et al., The application of jet fans to longitudinal tunnel ventilation. Paper presented at 6th Int. Symp. on Aerod. and Vent. of Vehicle Tunnels, Durham, England, Sept. 1988.
9. Anon., Measurement of fluid flow in closed conduits- Velocity area method using pitot static tubes, ISO 3966-1977.
10. Anon., Measurement of gas flow in conduits - Tracer methods -, Part I: General, ISO 4053/I-1977.

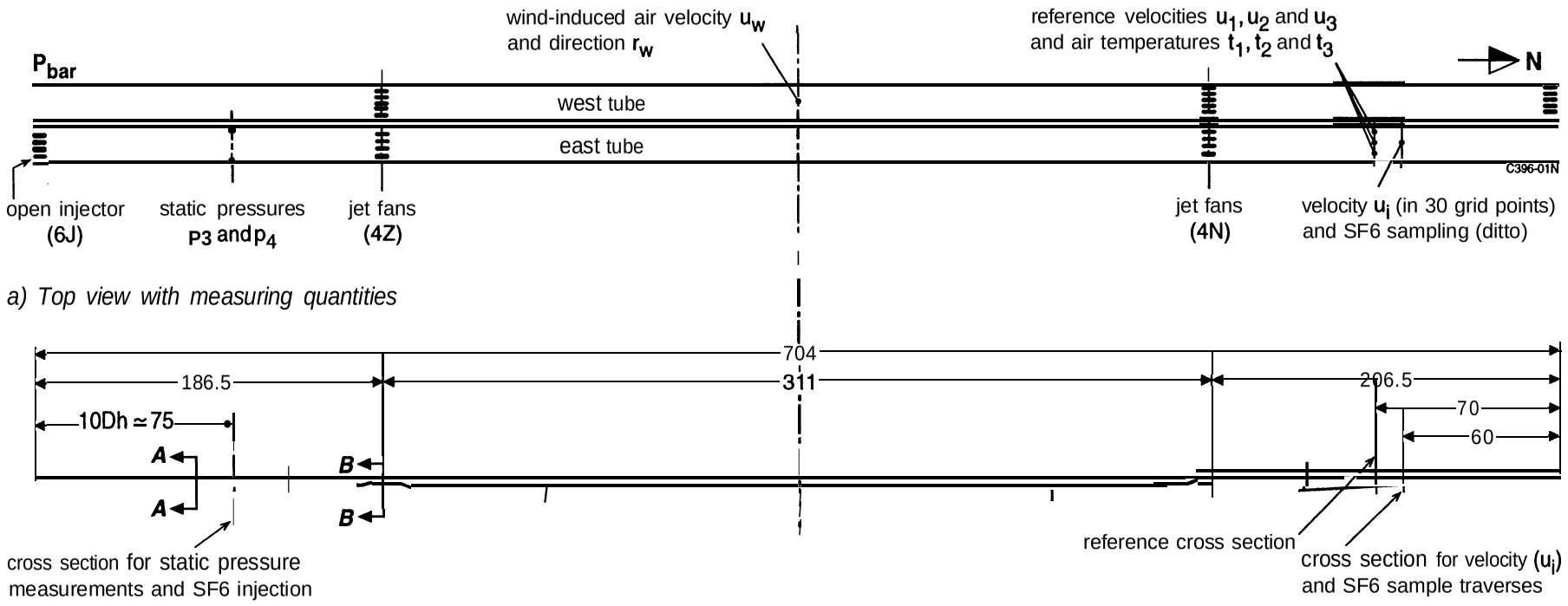

Fig. 1 Outline of set-up of measurements

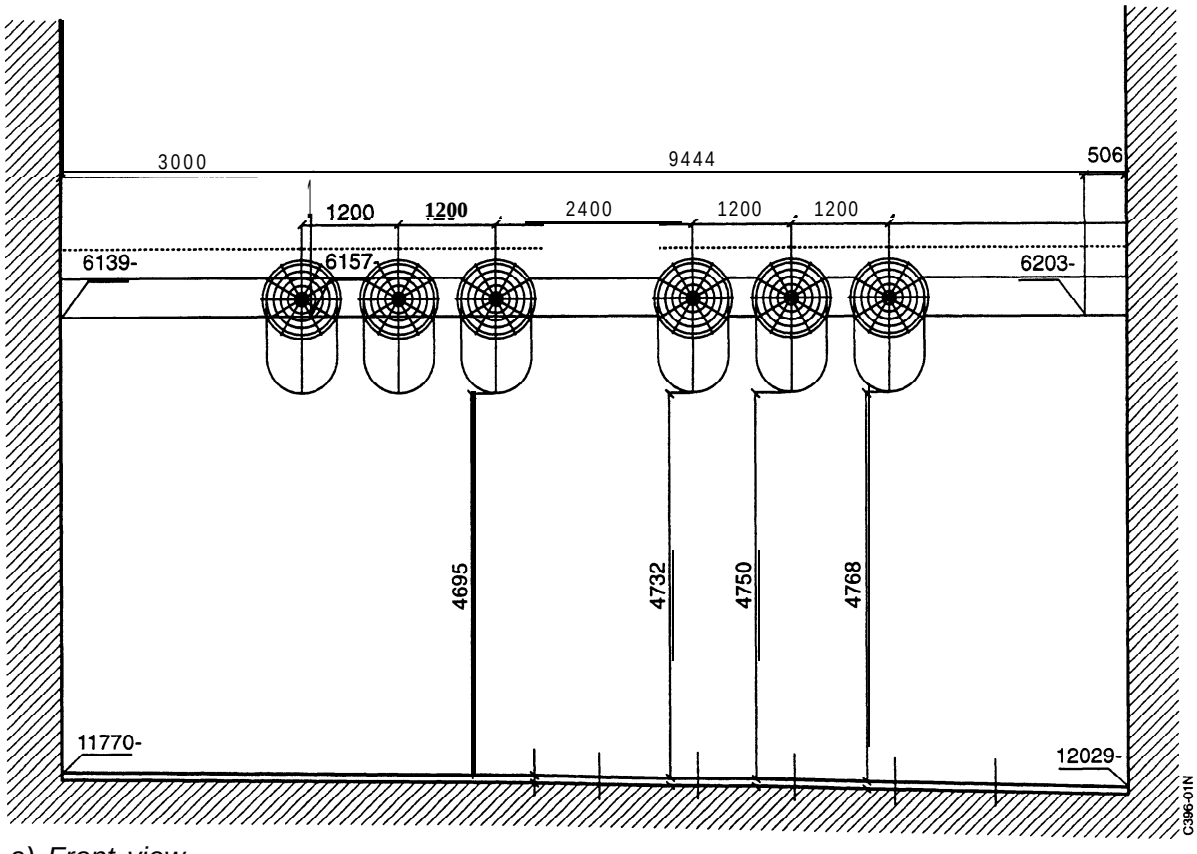

a) Front view

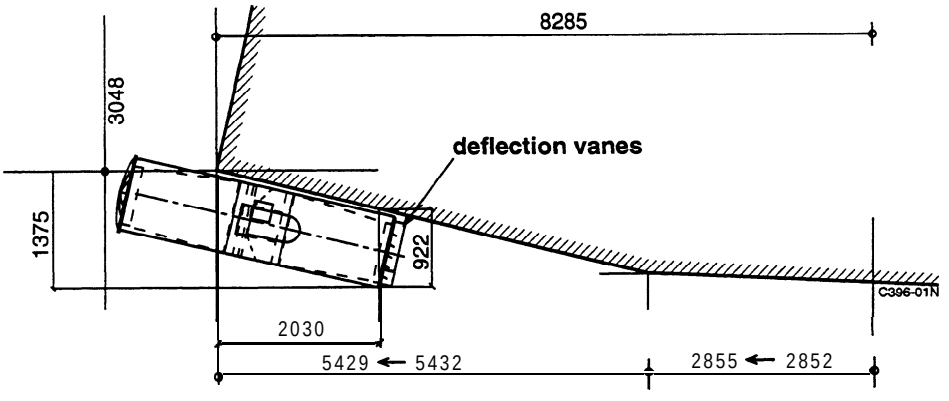

b) Side view

Fig. 2 The open injector at the entrance of the Wijkertunnel

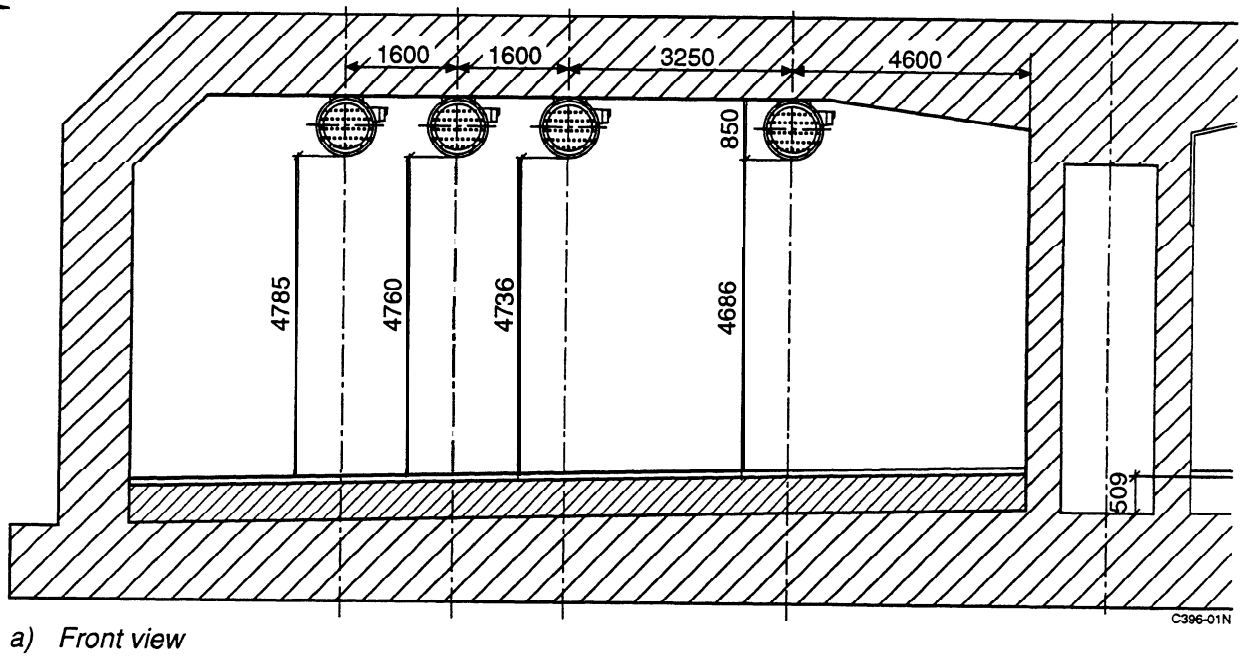

a) Front view

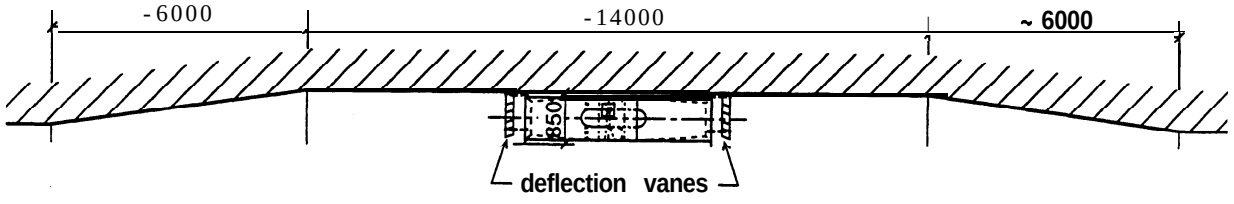

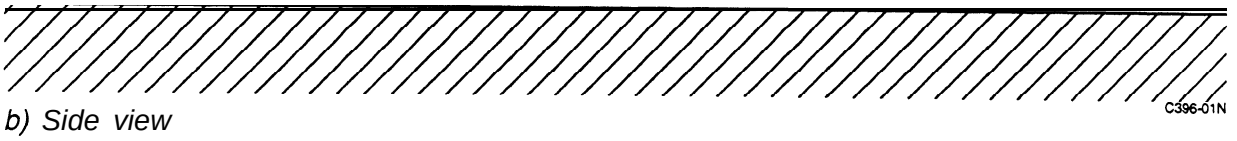

b) Side view

Fig. 3 One of the two groups of jet fans suspended in a niche of the east tube

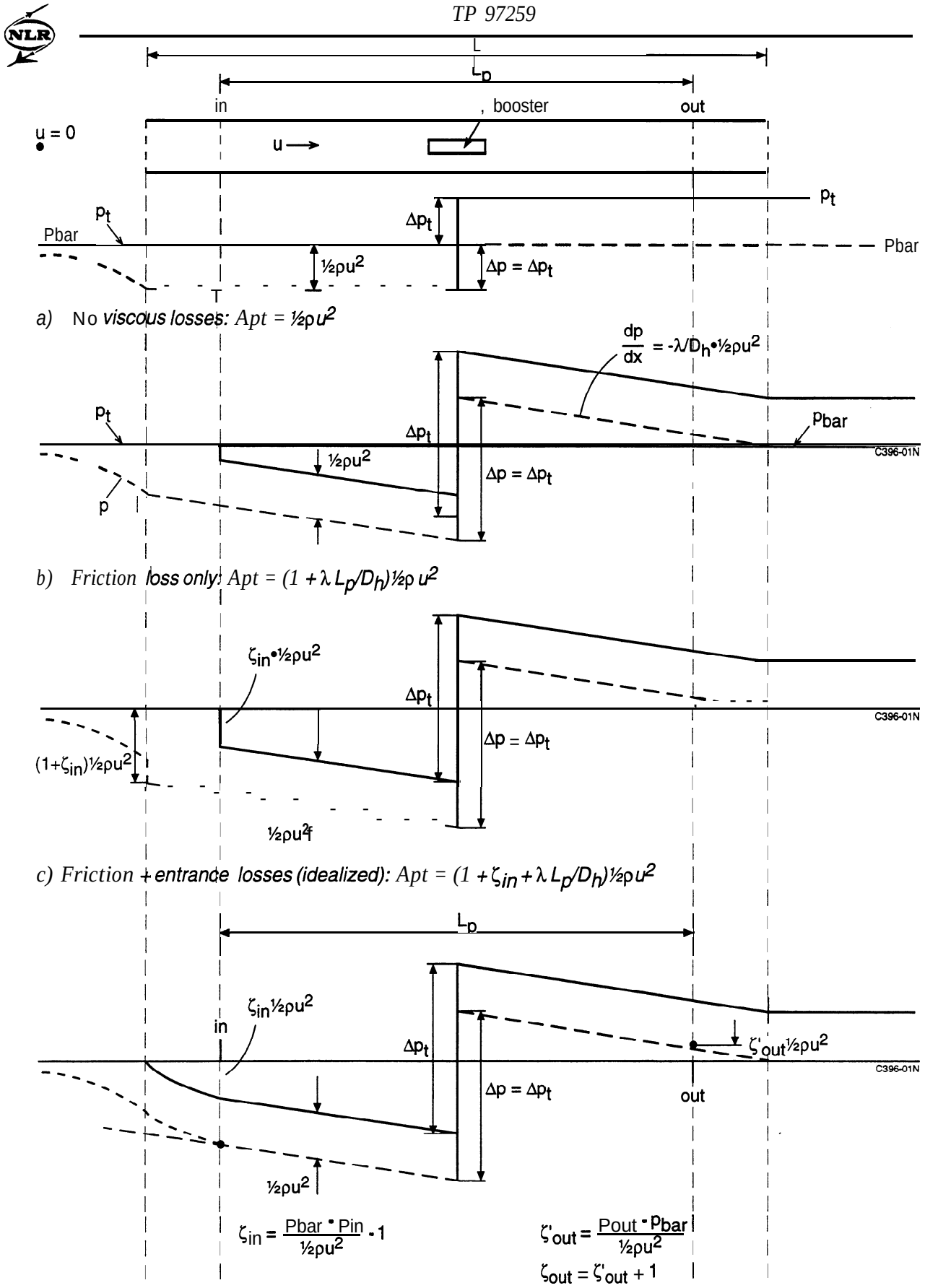

Fig. 4 Schematic presentation of static and total pressures along tunnel axis

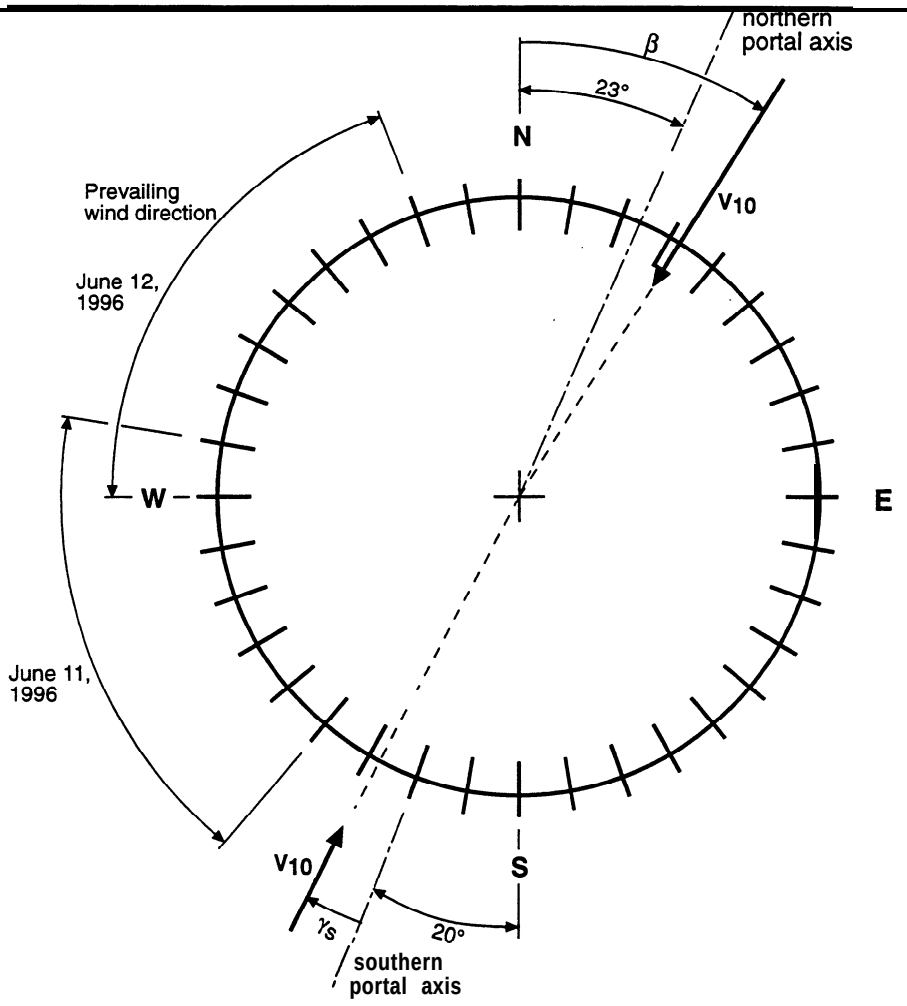

Fig. 5 Compass-card showing the definition of wind direction (angles β and γ_s) and the orientation of portal axes

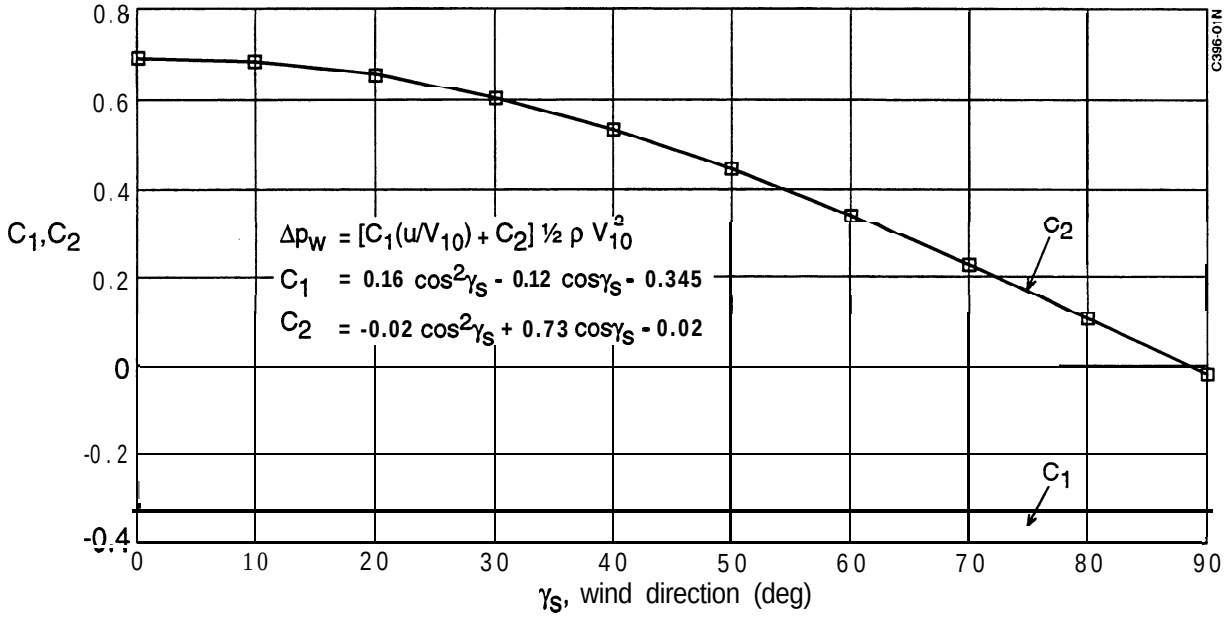

Fig. 6 Wind induced pressure difference $\Delta p_w = p_{in} - p_{out}$ as function of γ_s (Ref. 3)

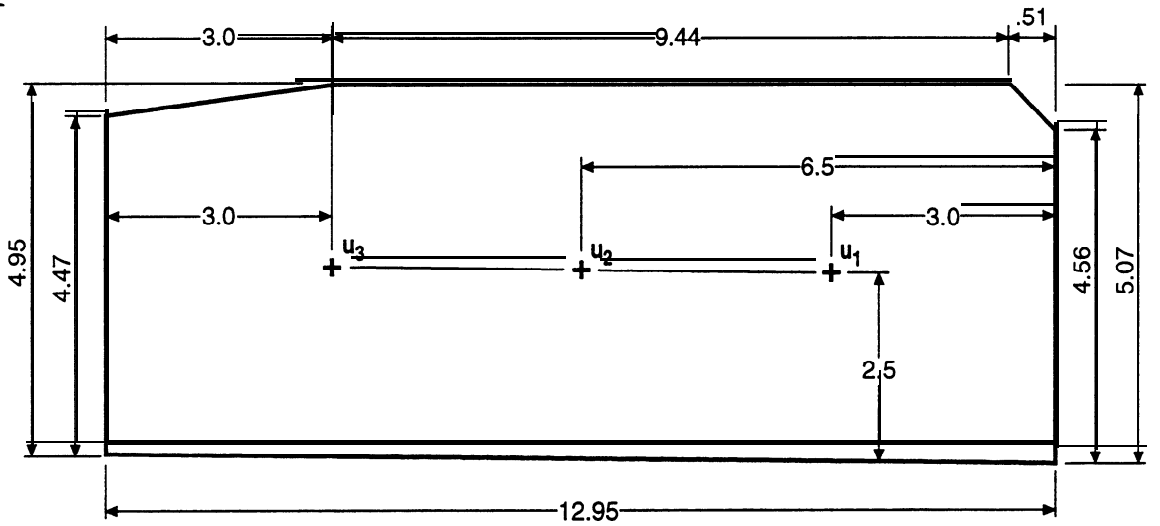

a) Nominal lateral dimensions of the east tube with measuring positions of u_1, u_2 and u_3

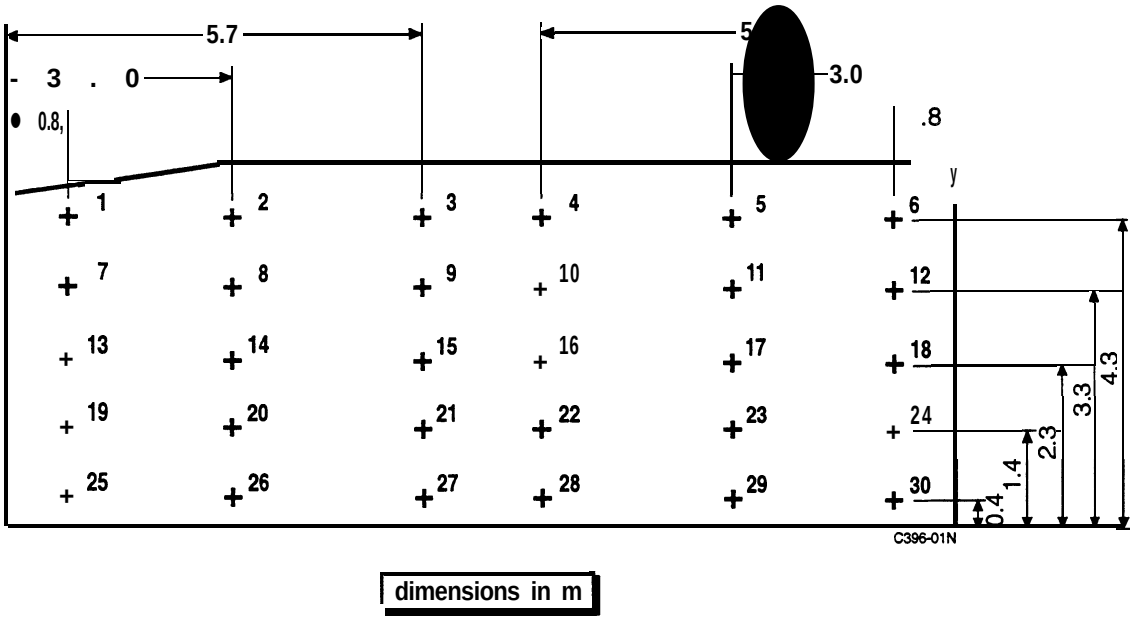

dimensions in m

b) Measuring points for u_i and SF6-sampling traverses

Fig. 7 The cross sections for velocity measurements in the east tube, viewed in northern direction

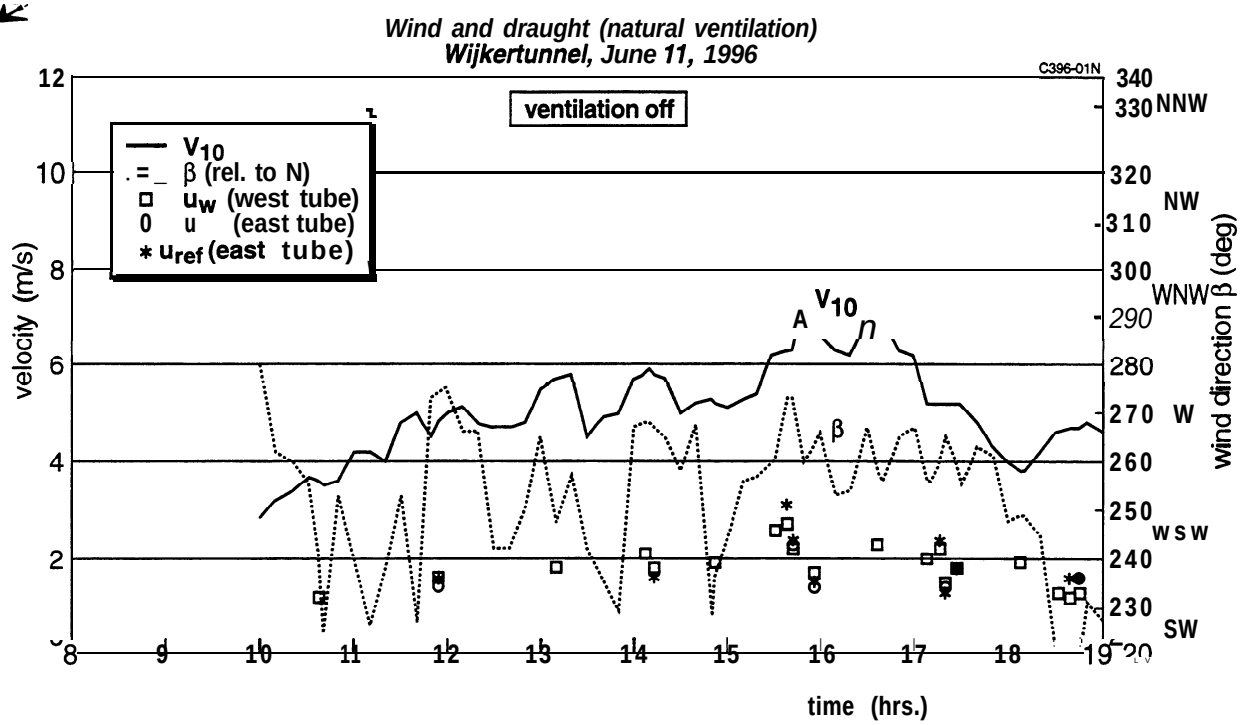

a) External wind conditions and air velocities in west and east tube on June 11, 1996

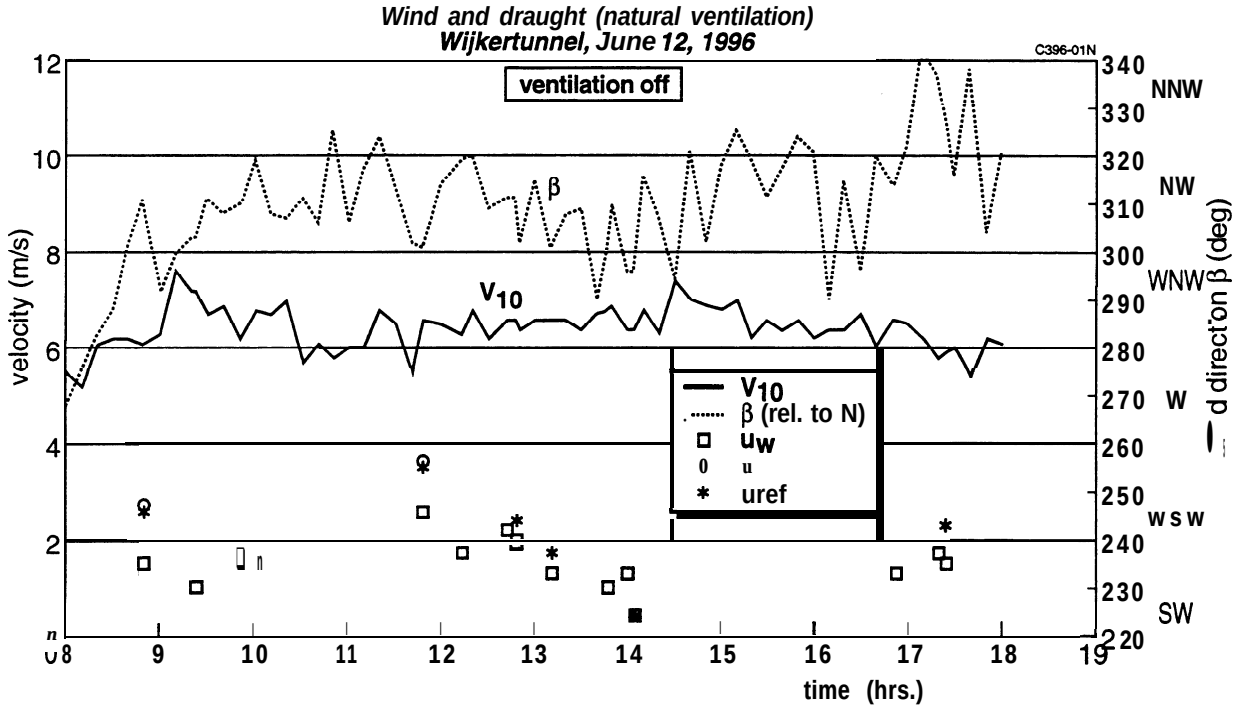

b) External wind conditions and air velocities in west and east tube on June 12, 1996

Fig. 8 External wind conditions compared with the air velocities in the tunnel without mechanical ventilation

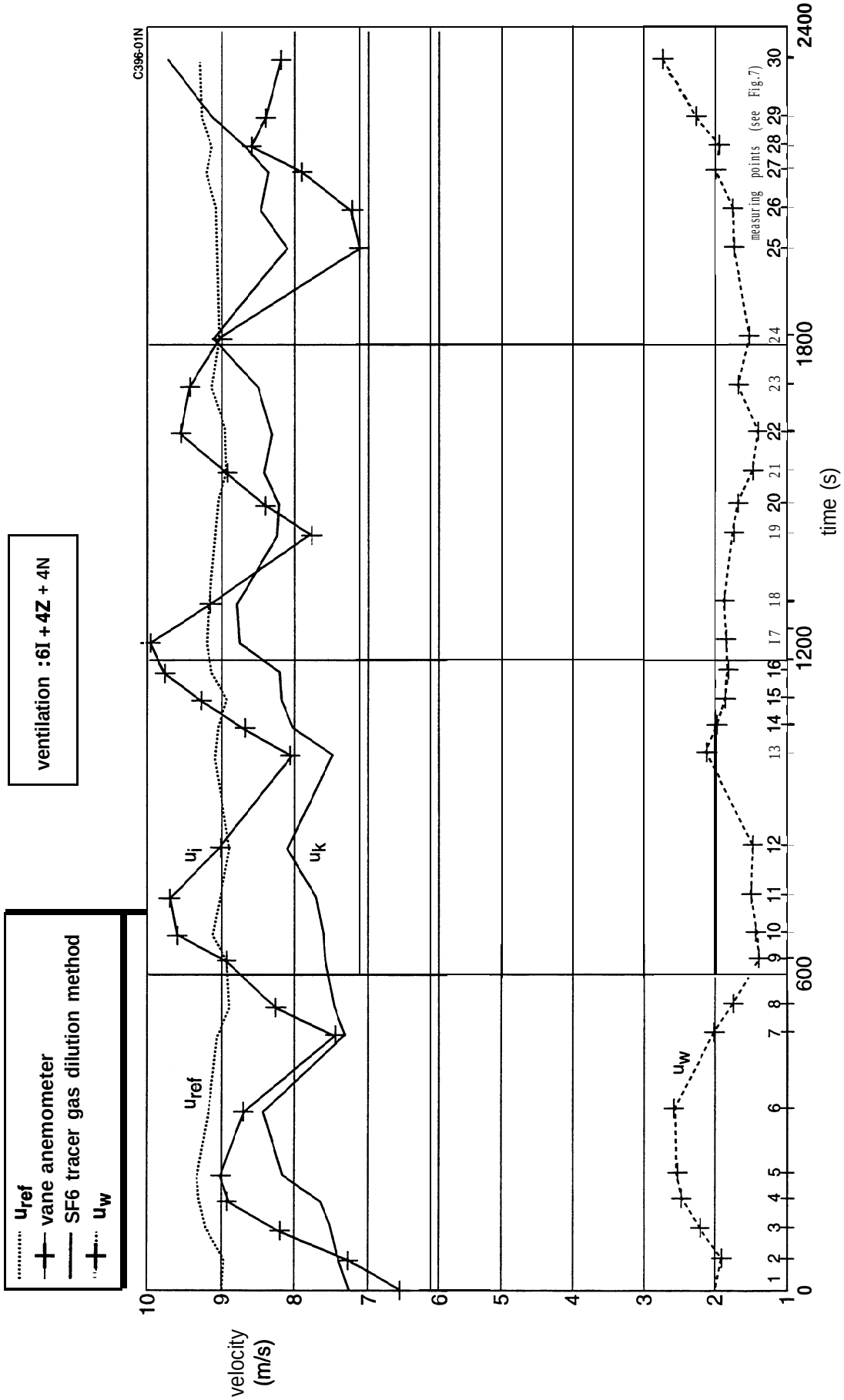

Fig. 9 Air velocities measured during traverse run 7